Observation of Vacuum-Induced Collective Quantum Beats

Hyok Sang Han,[1] Ahreum Lee,[1] Kanupriya Sinha,[2,5,*] Fredrik K. Fatemi,[3,4] and S. L. Rolston[1,4,†]
[1]Joint Quantum Institute, University of Maryland and the National Institute of Standards and Technology, College Park, Maryland 20742, USA
[2]Department of Electrical and Computer Engineering, Princeton University, Princeton, New Jersey 08544, USA
[3]U.S. Army Research Laboratory, Adelphi, Maryland 20783, USA
[4]Quantum Technology Center, University of Maryland, College Park, Maryland 20742, USA
[5]School of Electrical, Computer and Energy Engineering, Arizona State University, Tempe, Arizona 85287, USA

(Received 1 March 2021; accepted 2 July 2021; published 13 August 2021)

We demonstrate collectively enhanced vacuum-induced quantum beat dynamics from a three-level V-type atomic system. Exciting a dilute atomic gas of magneto-optically trapped ^{85}Rb atoms with a weak drive resonant on one of the transitions, we observe the forward-scattered field after a sudden shut-off of the laser. The subsequent radiative dynamics, measured for various optical depths of the atomic cloud, exhibits superradiant decay rates, as well as collectively enhanced quantum beats. Our work is also the first experimental illustration of quantum beats arising from atoms initially prepared in a single excited level as a result of the vacuum-induced coupling between excited levels.

DOI: 10.1103/PhysRevLett.127.073604

Introduction.—Quantum beats are a well-studied phenomenon that refers to the interference between spontaneously emitted radiation from two or more excited levels, resulting in a periodic modulation of the radiated field intensity [1]. This has been a valuable spectroscopic tool to measure the energy difference between excited levels across many experimental platforms such as atoms [2,3], molecules [4], semiconductors [5], and quantum dots [6,7].

Although quantum beats have been extensively studied, here we demonstrate two new aspects: (i) quantum beats without an initial superposition of excited levels, and (ii) enhanced beat amplitudes due to collective emission of light [8,9]. In a typical quantum beat experiment, an excitation pulse with sufficient bandwidth to span the energy spacing between multiple excited atomic levels is used to create an initial coherent superposition. The beat signal amplitude is proportional to the coherence between the excited levels; and in the absence of an initial superposition, one might expect no quantum beats. This notion was challenged in [10,11], predicting that the vacuum electromagnetic field can create the required coherence between the excited atomic levels. However, experimental observation of such vacuum-induced quantum beats is challenging due to the competing requirements on the level structure: The excited level's separation needs to be large compared to the natural linewidth to enable the initialization of only one of the levels that, in turn, reduces the strength of the vacuum-induced coupling.

We experimentally address this using the well-separated ^{85}Rb $^5P_{3/2}$ $F' = 3$ and 4 hyperfine levels as our excited levels and using a long enough (200 ns) excitation pulse such that any coherence due to the turn-on edge decays away, leaving the atomic population in a single excited level. Detecting the forward-scattered mode [see Fig. 1(a)] allows us to observe the radiation from a timed-Dicke state [12–14]. We theoretically illustrate that for such a collective state, the quantum beat dynamics can be cooperatively

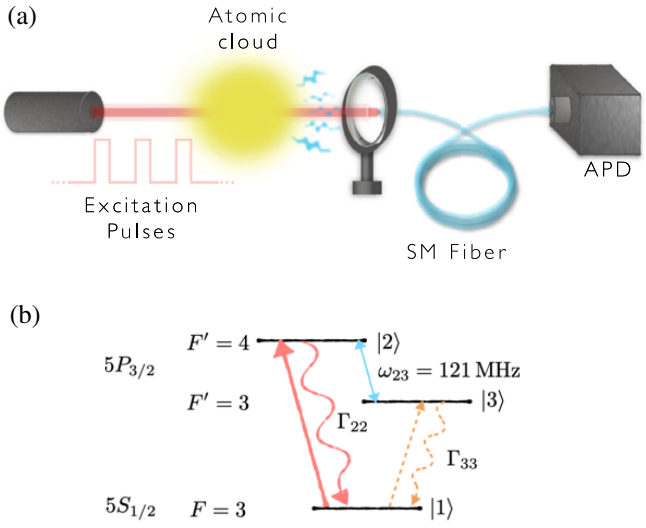

FIG. 1. (a) Experimental setup. Linearly polarized excitation beam containing train of pulses illuminates cold ^{85}Rb atomic cloud produced by MOT. Photons scattered by cloud in forward direction coupled into single-mode fiber, counted by avalanche photodiode, and histogrammed to obtain atomic radiative decay profile. (b) Relevant energy levels of ^{85}Rb atom. Excitation beam (780 nm) resonantly drives $|1\rangle \leftrightarrow |2\rangle$ transition. Γ_{22} and Γ_{33} are decay rates of excited levels $|2\rangle$ and $|3\rangle$, respectively, to ground level $|1\rangle$.

enhanced by the constructive interference between the transition processes in different atoms. The collective amplification of the forward-scattered beat signal allows us to observe vacuum-induced quantum beats and serves as an experimental proof of collective effects in quantum beats. Such collective enhancement may also be used to amplify small signals that are otherwise unobservable.

Model.—Let us consider a system of three-level V-type ^{85}Rb atoms, with the ground level $|1\rangle = |5S_{1/2}, F = 3\rangle$ and the two excited levels $|2\rangle = |5P_{3/2}, F' = 4\rangle$ and $|3\rangle = |5P_{3/2}, F' = 3\rangle$ [see Fig. 1(b)]. The frequency difference between the excited levels is $\omega_{23} = 2\pi \cdot 121$ MHz, and the optical transition wavelength between the ground and the excited levels is $\lambda = 780$ nm. We observe the forward scattering, where the phase factor of the field from propagation within the atomic cloud is exactly compensated for by the phases of the atomic dipoles initially induced by the drive [12]. The damping rate of atomic levels originating from second-order coupling between $|j\rangle$ and $|l\rangle$ is

$$\Gamma_{jl} = \frac{\vec{d}_{j1} \cdot \vec{d}_{l1} \omega_{j1}^3}{3\pi\varepsilon_0 \hbar c^3},$$

where $\vec{d}_{j1}$ and ω_{j1} are the transition dipole moments and the transition frequency between $|j\rangle$ and $|1\rangle$, respectively. Note that Γ_{23} represents the cross-damping rate between the excited states [11], whereas Γ_{22} and Γ_{33} describe the normal decay of the excited states. Assuming that all the transition dipole moments are real and parallel to each other, $\Gamma_{23} \approx \sqrt{\Gamma_{22}\Gamma_{33}}$. In our system, $\Gamma_{22} = 2\pi \cdot 6.1$ MHz is the single-atom decay rate of the $5P_{3/2}$ level and $\Gamma_{33} = (5/9)\Gamma_{22}$ because $|3\rangle$ decays to $|1\rangle$ only fractionally with the branching ratio of 5/9 [15].

The atoms are initialized in a symmetric state with a shared single excitation in $|2\rangle$. After a sudden turn-off of the drive field, the atomic ensemble starts to decay due to its interaction with the vacuum field modes, which couple the excited levels to reveal quantum beating. We analytically solve the atomic and field dynamics using the Wigner-Weisskopf theory in the experimental regime where the excited atomic levels are well separated from each other ($\Gamma_{jl}^{(N)} \ll \omega_{23}$) [16] to find the intensity of light emitted from the ensemble as (see Supplemental Material [17])

$$\frac{I(t)}{I_0} = e^{-\Gamma_{22}^{(N)} t} + I_b e^{-\Gamma_{\mathrm{avg}}^{(N)} t} \sin(\omega_{23} t + \phi), \tag{1}$$

where we have defined the total collective decay rate as $\Gamma_{jl}^{(N)} \equiv (1 + Nf)\Gamma_{jl}$, with f corresponding to the angular emission factor into the forward-scattered modes and N corresponding to the effective number of atoms emitting collectively [18]. We have assumed here that the atoms emit collectively in the forward direction as a result of the phase coherence due to the timed-Dicke state, whereas the emission in the remainder of the modes is independent. $\Gamma_{\mathrm{avg}}^{(N)} \equiv (\Gamma_{22}^{(N)} + \Gamma_{33}^{(N)})/2$ is the average decay rate of excited levels, the beat contrast is defined as

$$I_b = \frac{(\Gamma_{23}^{(N)})^2}{\omega_{23}\Gamma_{22}^{(N)}} \approx \frac{5}{9}\frac{\Gamma_{22}^{(N)}}{\omega_{23}}, \tag{2}$$

and the beat phase is defined as

$$\phi = \arctan\left(\frac{\Gamma_{22}^{(N)}}{\omega_{23}}\right). \tag{3}$$

The first term of Eq. (1) represents the collective decay from $|2\rangle$, with a cooperatively enhanced amplitude and decay rate relative to a single atom. The second term accounts for the small but non-negligible beat that decays away with an enhanced average rate of $\Gamma_{\mathrm{avg}}^{(N)}$. This result shows that vacuum-induced quantum beats in the absence of an initial superposition of excited atomic levels can exhibit collective effects, generalizing the single-atom quantum trajectory prediction in [11]. From Eq. (2), we observe that the collective nature of the quantum beat originates from the virtual coupling between the excited levels as indicated by the cross-damping term Γ_{23}.

Experiment.—Figure 1(a) shows the schematic of the experiment. A cold atomic cloud of $\sim 10^8$ ^{85}Rb atoms is produced by a magneto-optical trap (MOT) with Gaussian-shaped atomic density distribution having a $1/e$ diameter of ~ 2 mm. The ensemble satisfies the dilute regime, $\rho\lambda^3 \ll 1$, where ρ is the spatial atomic density, meaning that the separation between atoms is much larger than the photon wavelength. An excitation beam with a $1/e^2$ diameter of 1.6 mm is overlapped with the cloud whose transmitted light is collected by a single-mode (SM) fiber 0.6 m away in the forward direction.

For the observation of the spontaneous emission, the MOT lasers are turned off for 200 μs, during which atoms initialized in $|1\rangle$ are illuminated by a train of excitation pulses that resonantly drive the $|1\rangle \leftrightarrow |2\rangle$ transition. The peak intensity of the excitation beam is $\sim 6 \times 10^8$ times smaller than the saturation intensity of $I_s = 3.9$ mW/cm^2 of the transition [15], delivering less than one photon per pulse on average, and ensuring that the system is well within the single-excitation regime. Each excitation pulse is turned on (off) for 200 ns (800 ns) with > 30 dB extinction and a 3.5 ns fall time controlled by two fibered Mach-Zehnder intensity modulators (EOSPACE AZ-0K5-10-PFA-PFA-780) in series.

After the driving field is switched off, spontaneously emitted photons coupled to the SM fiber are counted by an avalanche photodiode and histogrammed by time tagging them with 0.5 ns resolution. By detecting only those

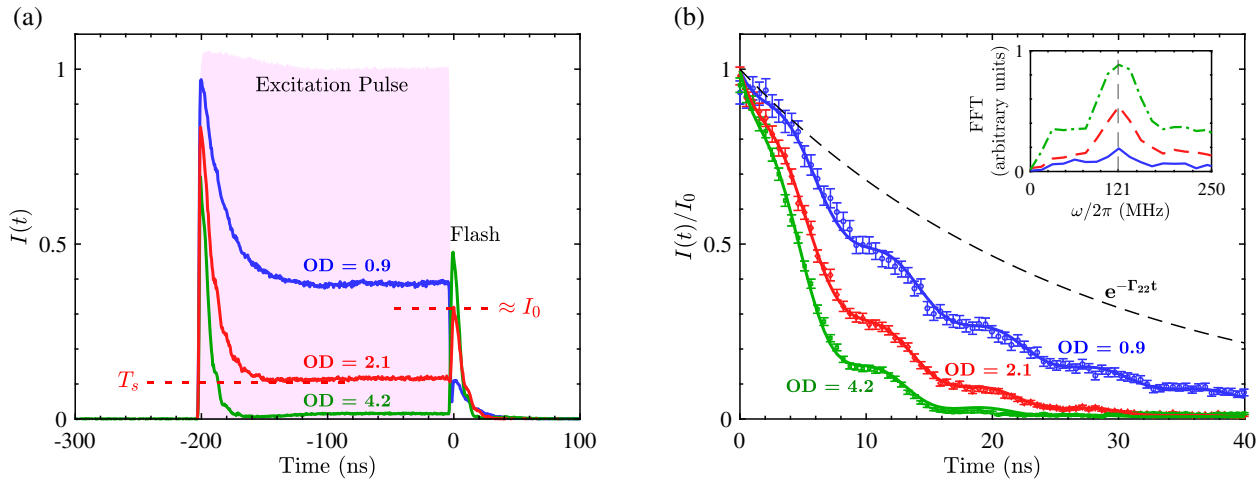

FIG. 2. (a) Examples of the histogrammed photon counts for various optical depths, representing forward-mode intensity, and normalized to that of excitation pulse. As excitation pulse is abruptly (within ≈3.5 ns) turned off, flash of photon emission occurs with peak intensity close to I_0. (b) Zoomed-in view of decay profiles after flash peak for analysis. Intensity of each curve further normalized to exponential decay amplitude I_0 [≈ flash peak size shown in Fig. 2(a)]. Error bars represent shot-noise limit of photon counts. Overlaid solid lines fit data using Eq. (1), whose results are displayed in Fig. 3 for entire OD range of experiment. Black dashed line represents single-atom decay curve $I(t) = e^{-\Gamma_{22}t}$ ($\Gamma_{22} = 2\pi \cdot 6.1$ MHz) without considering collective effects. In inset, absolute values of fast-Fourier transforms of beat signals for OD = 0.9 (solid blue), 2.1 (dashed red), and 4.2 (dash-dotted green line) show peaks at splitting between two excited levels (see Supplemental Material for detail [17]).

photons coupled to the SM fiber, we effectively filter out incoherent fluorescence, owing to the small collection solid angle ($\approx 6 \times 10^{-6}$ sr). The atomic velocity of $v \approx 120$ nm/μs corresponding to the Doppler temperature of $T_D \approx 150$ μK gives negligible motion compared to the optical wavelength (780 nm) within the timescale of the emission process ($1/\Gamma_{22}^{(N)} \leq 26$ ns). After the repetition of 200 pulses within 200 μs, the MOT lasers are turned back on to recover and maintain the atomic cloud for 1.8 ms before a new measurement cycle begins, repeating the whole sequence every 2 ms. For typical histogrammed data, we run the sequence continuously for 30 min, comprising 2×10^8 excitation pulses.

Examples of histogrammed photon counts are shown in Fig. 2(a), where $I(t)$ represents the intensity of the forward-scattered light normalized to the incident intensity. The atomic samples are almost transparent at the sharp switch-on edge of the excitation pulse due to its broad spectral components, but the transmission soon decays to a steady-state value T_s, which we use to calculate the optical depth (OD $= -\ln T_s$). We vary the OD of the MOT cloud between 0 and 5 by adjusting the injection current running through the rubidium dispensers (SAES Getters RB/NF/7/25) between 3.5 and 6.5 A to increase atomic background pressure. The steady-state transmission T_s results from the destructive interference between the driving field and the field coherently radiated (with π-phase shift) in the forward direction by the atomic dipoles. When the driving field is switched off, only the atomic radiation field remains in the forward direction, resulting in a sudden intensity jump ("flash"), which has been intensively investigated in previous studies [19–21]. The flash peak intensity, which is proportional to the OD before it saturates at OD ≈ 4, represents the intensity I_0 of the overall decay as in Eq. (1).

The decay profiles after the flash peak are magnified in Fig. 2(b) for detailed analysis. Each curve is normalized to the exponential decay amplitude I_0 [see Eq. (1)], and so the enhanced decay rates and the beat contrast for different ODs can be easily compared. For comparison, the single-atom decay curve of $I(t) = e^{-\Gamma_{22}t}$ with no collective enhancement is also shown (black dashed line). We first note that a higher OD results in an enhanced decay rate, demonstrating the collective nature of the emission process. The quantum beat signal is apparent as a sinusoidal modulation of the exponential decay. To verify the frequency of the observed beat signal, we first remove the exponential decay profile from the data and then fast-Fourier transform (FFT) the residual. The FFT results (see inset) confirm that the observed beat frequency is ω_{23}, as expected. This illustrates the occurrence of quantum beats in the absence of an initial superposition between the excited levels.

The solid curves overlaid with the experimental data in Fig. 2(b) represent the fitting of Eq. (1) with I_b, $\Gamma_{22}^{(N)}$, and ϕ as fitting parameters, showing excellent agreement between the analytical prediction and the observed emission dynamics. To preclude the possibility of exciting additional population in levels $|2\rangle$ and $|3\rangle$ due to the off-resonant Fourier components of the drive intensity, we numerically simulate the atomic dynamics via the optical Bloch equations (OBEs) by considering a realistic model for the laser dynamics with a 3.5 ns turn-on edge, a 200 ns drive, and a 3.5 ns turn-off edge (see Supplemental Material [17]). The emitted intensity curves calculated from the

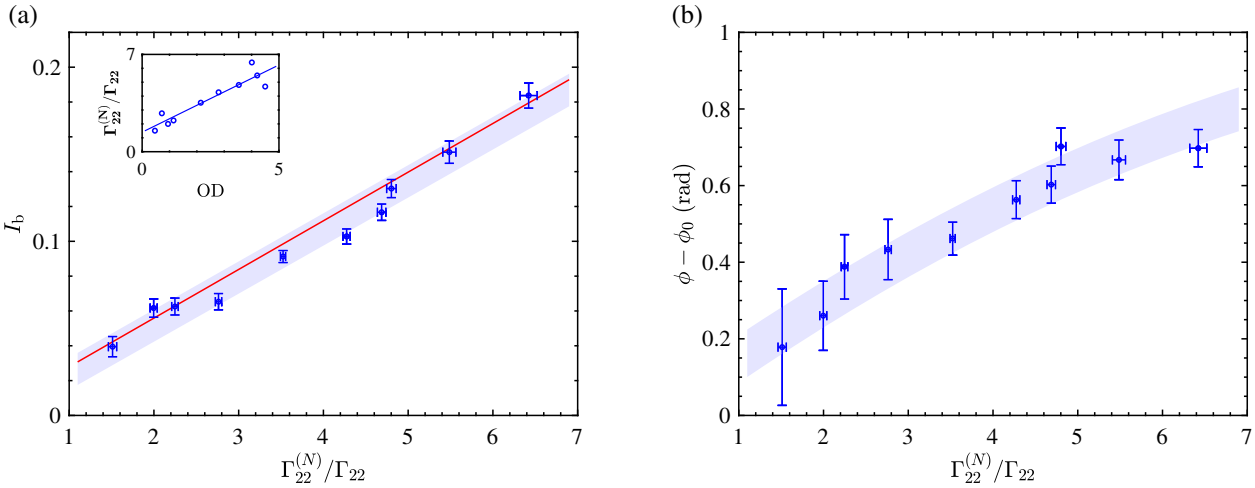

FIG. 3. (a) Beat contrast I_b plotted as function of $\Gamma_{22}^{(N)}/\Gamma_{22}$ for various ODs. Plotted error bars represent one-sigma confidence interval of fitting to modulated decay curves. Shaded region displays one-sigma confidence band of linear fit to data. Red solid line is theory curve plotting Eq. (2). Inset shows linear dependence of $\Gamma_{22}^{(N)}/\Gamma_{22}$ on OD. (b) Beat phase ϕ subtracted by common offset ϕ_0 presented. Shaded region represents one-sigma confidence band of fitting of Eq. (4) to data.

OBE dynamics are indistinguishable from the solid curves that represent the analytical Wigner-Weisskopf approach excluding the drive dynamics [Eq. (1)]. We therefore conclude that the off-resonant Fourier components associated with the turn-on and turn-off edges are sufficiently small that they do not cause an appreciable difference to the beat dynamics.

The data fitting of Eq. (1), the examples of which are presented in Fig. 2(b), is extended to the full experimental range of ODs between 0 and 5 as presented in Fig. 3. In the inset, the linear dependence of the enhancement factor $\Gamma_{22}^{(N)}/\Gamma_{22}$ on the OD displays the collective nature of the emission process, which is in agreement with the superradiant behavior [13,18,22–25]. The blue solid line fitting the data provides a linear relation $\Gamma_{22}^{(N)}/\Gamma_{22} = 1.0(1)\cdot\mathrm{OD} + 1.4(4)$, showing a qualitative agreement with the previous studies [26]. The beat contrast I_b is plotted as a function of $\Gamma_{22}^{(N)}/\Gamma_{22}$ in Fig. 3(a). The blue shaded region represents the one-sigma confidence band of the linear fit to the data, displaying the amplification of the quantum beat due to the increasing number of cooperative atoms. The red solid line plotting Eq. (2) is in good agreement with the data, confirming the validity of our model.

The measured beat phase ϕ is displayed in Fig. 3(b) and fit to

$$\phi = \arctan\left(\eta \cdot \frac{\Gamma_{22}^{(N)}}{\Gamma_{22}}\right) + \phi_0. \tag{4}$$

The fitted value of $\phi_0 = 0.17$ is presumably due to the transient intensity of the driving field during the switch-off time. From the fit, $\eta = 1.5(3) \times 10^{-1}$ is almost three times larger than its expected value of $\Gamma_{22}/\omega_{23} = 5.0 \times 10^{-2}$ [see Eq. (3)]. We note that nonequilibrium dynamics during the switch-off time can produce an additional OD-dependent phase delay, potentially resulting in a larger η value than expected, which is not captured by our current model. Such an additional phase can be used to characterize the nonequilibrium dynamics of emission during the transient time, the study of which is left to future work.

Discussion.—We have demonstrated collective quantum beats in a spontaneous emission process without an initial superposition of the excited levels in a three-level atomic system. The collective nature of the forward emission results in an enhanced coupling between the excited levels, which is manifested in cooperatively amplified quantum beats. We observe that the enhancement factor $\Gamma_{22}^{(N)}/\Gamma_{22}$ for the collective decay rate increases with the atomic OD. The beat contrast also scales with $\Gamma_{22}^{(N)}/\Gamma_{22}$, in agreement with our theoretical prediction. It signifies a combination of two different quantum interference phenomena featuring interplay between multilevel atomic structure and multiatom collective effects, which have been the focus of many theoretical studies [27–29].

The collective enhancement of quantum beats can be a valuable tool in precision spectroscopy by enhancing beat amplitudes in systems with small signals. It can also be utilized as a source of strongly correlated photons. For example, previous works have illustrated that a system of three-level V-type atoms in an interferometric setup, as in the case of a "quantum beat laser" [30,31], can exhibit strong correlations in the two-frequency emission [32,33]. It has been suggested as a means of generating or amplifying entanglement in the radiated field modes [34,35]. These proposed schemes rely on the coherence between the excited atomic levels, therefore requiring a strong classical drive to induce such coherences.

Vacuum-induced collective quantum beats can circumvent the need for a classical drive, thereby avoiding additional noise, while facilitating a collective signal enhancement.

Our study of collective quantum effects can be readily combined with waveguide optics to study interactions between distant atomic ensembles [36–42]. Recent studies have shown that such delocalized collective states can exhibit surprisingly rich non-Markovian dynamics [43–50]. A challenge in observing such exotic dynamics is that the quantum optical correlation between the multiple emitters is highly sensitive to the position of individual atoms, requiring subwavelength precision. Replacing the optical frequency by the beat radio frequency could allow one to bypass the strict requirements on controlling the atomic positions. An experimental investigation of collective effects in non-Markovian regimes with multilevel atomic ensembles coupled to optical nanofibers is within the scope of our future works [42].

The supporting data for this Letter are openly available from D. A. Steck's Alkali D Line Data suppository [15].

We thank Hyun Gyung Lee and Huan Q. Bui for technical support and fruitful discussions. We are also grateful to Pablo Solano and Jonathan Hoffman for helpful comments. This research is supported by the U.S. Army Research Laboratory's Maryland ARL Quantum Partnership (W911NF-19-2-0181) and the Joint Quantum Institute (70NANB16H168).

H. S. H. and A. L. contributed equally to this work.

*kanu@princeton.edu
†rolston@umd.edu

[1] E. T. Jaynes, in *Foundations of Radiation Theory and Quantum Electrodynamics*, edited by A. O. Barut (Springer US, Boston, MA, 1980), p. 37.
[2] S. Haroche, J. A. Paisner, and A. L. Schawlow, Phys. Rev. Lett. **30**, 948 (1973).
[3] C. G. Wade, N. Šibalić, J. Keaveney, C. S. Adams, and K. J. Weatherill, Phys. Rev. A **90**, 033424 (2014).
[4] E. Hack and J. R. Huber, Int. Rev. Phys. Chem. **10**, 287 (1991).
[5] H. Stolz, V. Langer, E. Schreiber, S. Permogorov, and W. von der Osten, Phys. Rev. Lett. **67**, 679 (1991).
[6] I. E. Kozin, V. G. Davydov, I. V. Ignatiev, A. V. Kavokin, K. V. Kavokin, G. Malpuech, H.-W. Ren, M. Sugisaki, S. Sugou, and Y. Masumoto, Phys. Rev. B **65**, 241312(R) (2002).
[7] J. Bylsma, P. Dey, J. Paul, S. Hoogland, E. H. Sargent, J. M. Luther, M. C. Beard, and D. Karaiskaj, Phys. Rev. B **86**, 125322 (2012).
[8] R. H. Dicke, Phys. Rev. **93**, 99 (1954).
[9] M. Gross and S. Haroche, Phys. Rep. **93**, 301 (1982).
[10] G. C. Hegerfeldt and M. B. Plenio, Phys. Rev. A **47**, 2186 (1993).
[11] G. C. Hegerfeldt and M. B. Plenio, Quantum Opt. **6**, 15 (1994).
[12] M. O. Scully, E. S. Fry, C. H. R. Ooi, and K. Wódkiewicz, Phys. Rev. Lett. **96**, 010501 (2006).
[13] T. Bienaimé, R. Bachelard, N. Piovella, and R. Kaiser, Fortschr. Phys. **61**, 377 (2013).
[14] S. L. Bromley, B. Zhu, M. Bishof, X. Zhang, T. Bothwell, J. Schachenmayer, T. L. Nicholson, R. Kaiser, S. F. Yelin, M. D. Lukin, A. M. Rey, and J. Ye, Nat. Commun. **7**, 11039 (2016).
[15] D. A. Streck, Data for "Rubidium 85D Line Data," Revision 2.2.1, Alkali D Line Data, http://steck.us/alkalidata (21 Nov. 2019).
[16] Although the vacuum-induced quantum beats are a second-order process, we note that the population in the excited level $|3\rangle$ depends on the relative strength of the cross-damping coefficient to the excited level separation, $|c_3(t)| \sim \Gamma_{23}/\omega_{23}$ (see Supplemental Material for details [17]), making the contribution non-negligible.
[17] See Supplemental Material at http://link.aps.org/supplemental/10.1103/PhysRevLett.127.073604 for derivation of the theoretical model and data analysis.
[18] M. O. Araújo, I. Krešić, R. Kaiser, and W. Guerin, Phys. Rev. Lett. **117**, 073002 (2016).
[19] M. Chalony, R. Pierrat, D. Delande, and D. Wilkowski, Phys. Rev. A **84**, 011401(R) (2011).
[20] C. C. Kwong, T. Yang, M. S. Pramod, K. Pandey, D. Delande, R. Pierrat, and D. Wilkowski, Phys. Rev. Lett. **113**, 223601 (2014).
[21] C. C. Kwong, T. Yang, D. Delande, R. Pierrat, and D. Wilkowski, Phys. Rev. Lett. **115**, 223601 (2015).
[22] T. Bienaimé, M. Petruzzo, D. Bigerni, N. Piovella, and R. Kaiser, J. Mod. Opt. **58**, 1942 (2011).
[23] T. Bienaimé, N. Piovella, and R. Kaiser, Phys. Rev. Lett. **108**, 123602 (2012).
[24] S. J. Roof, K. J. Kemp, M. D. Havey, and I. M. Sokolov, Phys. Rev. Lett. **117**, 073003 (2016).
[25] W. Guerin, M. T. Rouabah, and R. Kaiser, J. Mod. Opt. **64**, 895 (2017).
[26] See, for example, equation 4 in [18]. The previously predicted value (1/12) of the ratio between the collective decay rate enhancement and the OD is different from our measured value of 1.0(1). We remark that our experimental characteristics, such as the atomic density distribution or detection solid angle, may have caused a deviation from the analytical prediction [22].
[27] G. S. Agarwal, Phys. Rev. A **15**, 2380 (1977).
[28] G. S. Agarwal and A. K. Patnaik, Phys. Rev. A **63**, 043805 (2001).
[29] W. W. Chow, M. O. Scully, and J. O. Stoner, Phys. Rev. A **11**, 1380 (1975).
[30] M. O. Scully, Phys. Rev. Lett. **55**, 2802 (1985).
[31] M. O. Scully and M. S. Zubairy, Phys. Rev. A **35**, 752 (1987).
[32] M. Ohtsu and K. Y. Liou, Appl. Phys. Lett. **52**, 10 (1988).
[33] M. P. Winters, J. L. Hall, and P. E. Toschek, Phys. Rev. Lett. **65**, 3116 (1990).
[34] H. Xiong, M. O. Scully, and M. S. Zubairy, Phys. Rev. Lett. **94**, 023601 (2005).

[35] S. Qamar, F. Ghafoor, M. Hillery, and M. S. Zubairy, Phys. Rev. A **77**, 062308 (2008).
[36] D. E. Chang, V. Vuletić, and M. D. Lukin, Nat. Photonics **8**, 685 (2014).
[37] E. Vetsch, D. Reitz, G. Sagué, R. Schmidt, S. T. Dawkins, and A. Rauschenbeutel, Phys. Rev. Lett. **104**, 203603 (2010).
[38] A. Goban, K. S. Choi, D. J. Alton, D. Ding, C. Lacroûte, M. Pototschnig, T. Thiele, N. P. Stern, and H. J. Kimble, Phys. Rev. Lett. **109**, 033603 (2012).
[39] A. Goban, C.-L. Hung, J. D. Hood, S.-P. Yu, J. A. Muniz, O. Painter, and H. J. Kimble, Phys. Rev. Lett. **115**, 063601 (2015).
[40] S.-P. Yu, J. D. Hood, J. A. Muniz, M. J. Martin, R. Norte, C.-L. Hung, S. M. Meenehan, J. D. Cohen, O. Painter, and H. J. Kimble, Appl. Phys. Lett. **104**, 111103 (2014).
[41] A. Goban, C.-L. Hung, S.-P. Yu, J. D. Hood, J. A. Muniz, J. H. Lee, M. J. Martin, A. C. McClung, K. S. Choi, D. E. Chang, O. Painter, and H. J. Kimble, Nat. Commun. **5**, 3808 (2014).
[42] P. Solano, J. A. Grover, J. E. Hoffman, S. Ravets, F. K. Fatemi, L. A. Orozco, and S. L. Rolston, Adv. At. Mol. Opt. Phys. **66**, 439 (2017).
[43] H. Pichler and P. Zoller, Phys. Rev. Lett. **116**, 093601 (2016).
[44] F. Dinc, İ. Ercan, and A. M. Brańczyk, Quantum **3**, 213 (2019).
[45] F. Dinc and A. M. Brańczyk, Phys. Rev. Research **1**, 032042 (R) (2019).
[46] A. Carmele, N. Nemet, V. Canela, and S. Parkins, Phys. Rev. Research **2**, 013238 (2020).
[47] K. Sinha, P. Meystre, E. A. Goldschmidt, F. K. Fatemi, S. L. Rolston, and P. Solano, Phys. Rev. Lett. **124**, 043603 (2020).
[48] K. Sinha, P. Meystre, and P. Solano, in *Quantum Nanophotonic Materials, Devices, and Systems 2019*, edited by C. Soci, M. T. Sheldon, and M. Agio (11091, SPIE, Bellingham, 2019), p. 53.
[49] G. Calajó, Y.-L. L. Fang, H. U. Baranger, and F. Ciccarello, Phys. Rev. Lett. **122**, 073601 (2019).
[50] K. Sinha, A. González-Tudela, Y. Lu, and P. Solano, Phys. Rev. A **102**, 043718 (2020).